Food and Chemical Toxicology 85 (2015) 61–70

Contents lists available at ScienceDirect

Food and Chemical Toxicology

journal homepage: www.elsevier.com/locate/foodchemtox

ZnO nanoparticles induced inflammatory response and genotoxicity in human blood cells: A mechanistic approach

Violet Aileen Senapati [a, b], Ashutosh Kumar [a], Govind Sharan Gupta [a], Alok Kumar Pandey [b, **], Alok Dhawan [a, b, *]

[a] Institute of Life Sciences, School of Science and Technology, Ahmedabad University, University Road, Ahmedabad 380009, Gujarat, India
[b] CSIR-Indian Institute of Toxicology Research, Mahatma Gandhi Marg, P.O. Box 80, Lucknow 226001, Uttar Pradesh, India

ARTICLE INFO

Article history:
Received 29 April 2015
Received in revised form
26 June 2015
Accepted 27 June 2015
Available online 2 July 2015

Keywords:
Zinc oxide nanoparticles
Cellular uptake
Cytokines
Oxidative stress
Immunotoxicity

ABSTRACT

The wide application of zinc oxide nanoparticles (ZnO NPs) in cosmetics, paints, biosensors, drug delivery, food packaging and as anticancerous agents has increased the risk of human exposure to these NPs. Earlier *in vitro* and *in vivo* studies have demonstrated a cytotoxic and genotoxic potential of ZnO NPs. However, there is paucity of data regarding their immunomodulatory effects. Therefore, the present study was aimed to investigate the immunotoxic potential of ZnO NPs using human monocytic cell line (THP-1) as model to understand the underlying molecular mechanism. A significant ($p < 0.01$) increase in pro-inflammatory cytokines (TNF-α and IL-1β) and reactive oxygen species (ROS) was observed with a concomitant concentration dependent (0.5, 1, 5, 10, 15 and 20 μg/mL) decrease in the glutathione (GSH) levels as compared to control. The expression levels of mitogen activated protein kinase (MAPK) cascade proteins such as p-ERK1/2, p-p38 and p-JNK were also significantly ($p < 0.05$, $p < 0.01$) induced. Also, at the concentration tested, NPs induced DNA damage as assessed by the Comet and micronucleus assays. Our data demonstrated that ZnO NPs induce oxidative and nitrosative stress in human monocytes, leading to increased inflammatory response via activation of redox sensitive NF-κB and MAPK signalling pathways.

1. Introduction

Nanotechnology is an enabling technology due to the applications of nanoparticles (NPs) in diverse commercial products like paints, sunscreens, drug delivery systems, genetic engineering and other therapeutics. Metal oxide NPs have attracted enormous scientific and technological interest, mainly due to their unique size dependent properties that allow their use as active materials in food, cosmetic, clothing, and in biomedical areas (Johnston et al., 2010; Kreuter and Gelperina, 2008).

Nanomaterials including ZnO NPs are being explored for the use in medicine, biosensors, laboratory diagnostics, nanoscale devices for drug delivery and as antimicrobial agents (Fortina et al., 2007; Hanley et al., 2008; Patel et al., 2014; Wang et al., 2006). The total US market for nanomedicines is expected to sustain a strong upward pace to $118 billion in 2019 (Nanotechnology, 2010).

ZnO is considered to be a "GRAS" (generally recognized as safe) substance by the US Food and Drug Administration (Rasmussen et al., 2010). This holds true for materials in the micron to larger size range. However, when their size is reduced to nanoscale, it can result in adverse effect to human health (Rasmussen et al., 2010). This has been attributed to the fact that as the size is reduced, there is a corresponding increase in the surface area per unit mass (Kumar et al., 2014; Oberdorster et al., 2005). ZnO NPs have been shown to elicit cytotoxic and genotoxic responses in various organ specific cell lines, such as murine blood macrophages, human epidermal cells and others (Hong et al., 2013; Sharma et al., 2009). In an *in vivo* study, ZnO NPs have been shown to adversely affect the liver, kidney, lung, spleen, and pancreas (Hong et al., 2013).

In humans, NPs are first recognized by the cells of the immune system (e.g. monocytes) and their undesirable interactions may

* Corresponding author. Institute of Life Sciences, School of Science and Technology, Ahmedabad University, University Road, Ahmedabad 380009, Gujarat, India.
** Corresponding author. Nanomaterial Toxicology Group, CSIR-Indian Institute of Toxicology Research, Mahatma Gandhi Marg, P.O. Box 80, Lucknow 226001, Uttar Pradesh, India.
E-mail addresses: alokpandey@iitr.res.in (A.K. Pandey), alok.dhawan@ahduni.edu.in (A. Dhawan).

http://dx.doi.org/10.1016/j.fct.2015.06.018
0278-6915/

lead to immunostimulation or immunosuppression, inflammatory or autoimmune disorders, infections and cancer (Zolnik et al., 2010). Immune system can even engulf and eliminate certain NPs (Dobrovolskaia et al., 2008). The prime function of the immune system is to protect the host from threats caused by toxic substances and pathogens. However, inadvertent recognition of NPs as a toxin, by the immune cells may result in a multilevel immune response against the NPs and eventually lead to immune activation. There are conflicting results in the literature regarding the inflammatory potential of ZnO NPs (Roy et al., 2011; Xia et al., 2008). Studies have also demonstrated that generation of ROS and oxidative stress is the key mechanism in NP-induced toxicity (Park and Park, 2009; Premanathan et al., 2011); however, the role of cytokines is not well understood.

In this study, we have addressed the relationship between ZnO NPs immunotoxicity, oxidative stress and MAPK proteins. We have also assessed whether the inflammatory response plays any role in genotoxicity of ZnO NPs. To achieve these aims we have exposed human THP-1 monocytes to a range of concentration of ZnO NPs. THP-1 cells are preferred over human primary monocytes—macrophages as primary cells have the tendency to lose their characteristics under *in vitro* culture conditions over a period of time and hence pose problems with results reproducibility (Ekwall et al., 1990). Hence, in the present study it was found prudent to use THP-1 cells to understand the mechanism of immunotoxicity of ZnO NPs.

We have examined the cytokines release on ZnO NPs exposure along with the generation of ROS and alteration in GSH levels. Comet and Cytokinesis-block micronucleus (CBMN) assays determined the link between genotoxicity and inflammatory response. Finally the role of MAPK proteins and transcription factor nuclear factor kappa-light-chain-enhancer of activated B cells (NF-κB) has been elucidated.

We therefore designed the present study to address the immunomodulatory effects of ZnO NPs and also to unravel the mechanism of inflammatory response.

2. Materials and methods

2.1. Chemicals

Zinc oxide nanopowder (purity > 99%), low melting point agarose, normal melting agarose, ethidium bromide (EtBr), triton X-100 and poly-L-lysine (PLL) were purchased from Sigma Chemical Co. Ltd. (St. Louis, MO, USA). Ethylenediaminetetraacetic acid (EDTA) disodium salt was procured from Hi-media Pvt. Ltd. (Mumbai, MH India). Foetal bovine serum (FBS), Roswell Park Memorial Institute (RPMI) 1640 media, antibiotic and antimycotic solution (10,000 U/mL penicillin, 10 mg/mL streptomycin, 25 μg/mL amphotericin B), phosphate buffered saline (PBS; Ca^{2+}, Mg^{2+} free) were purchased from Life Technologies (India) Pvt. Ltd. (New Delhi, India). Cell culture plastic wares were purchased from Thermo Fisher Scientific Nunc (Rochester, NY, USA).

2.2. Preparation and characterization of ZnO NPs

ZnO NPs were suspended in RPMI medium supplemented with 10% FBS at a concentration of 100 μg/mL and probe sonicated (Sonics Vibra cell, Sonics & Material Inc., New Town, USA) at 32 W for 4 min (1 min on and 30 s off).

The size of ZnO NPs was determined by transmission electron microscope (TEM; Technai™ G2 Spirit, FEI Company, The Netherlands) by drop coating the stock suspension (100 μg/mL in Milli-Q water) on formvar coated copper grids and scanned at an accelerating voltage of 80 kV.

The size was also determined by scanning electron microscopy (SEM; Quanta FEG 450, FEI Company, The Netherlands) by taking ZnO NPs powder on carbon tape.

The average hydrodynamic size and zeta potential of ZnO NPs suspension was determined by dynamic light scattering (DLS) and phase analysis light scattering respectively using a Zetasizer Nano-ZS equipped with 4.0 mW, 633 nm laser (Model ZEN3600, Malvern instruments Ltd., Malvern, UK).

2.3. Cell culture and exposure to ZnO NPs

The human monocytic cell line, THP-1 was obtained from National Centre for Cell Sciences (NCCS), Pune, India. Cells were cultured in RPMI 1640 medium supplemented with 10% FBS, 10 mL/L of antibiotic and antimycotic solution at 37 °C under humidified conditions with 5% CO_2 in cell culture incubator. Cells were plated in 96, 24, 12, 6 well culture plates, and 25 cm^2 culture flask having a volume of 0.1, 0.5, 1, 2 and 5 mL respectively according to the experiments and were treated with different concentrations (0.5, 1, 5, 10, 15 and 20 μg/mL) of ZnO NPs in media at 37 °C for different time intervals.

2.4. Cellular internalization of ZnO NPs

2.4.1. Flow cytometry

The uptake of ZnO NPs in THP-1 cells was determined by flow cytometry according to the method of Suzuki et al. (2007). This method is based on the principle that the increase in intensity of side scattered (SSC) light with constant intensity of forward scattered (FSC) light in cells reveals increased granularity of cells which is correlated to cellular uptake of NPs. SSC is defined as the laser light scattered at about a 90° angle to the axis of the laser beam while FSC is the laser light scattered at narrow angles to the axis of laser beam. Briefly 2×10^5 cells were treated with different concentrations (0.5, 1, 5, 10, 15 and 20 μg/mL) of ZnO NPs for 6 h. After treatment, cells were washed with 1 x PBS and the samples were evaluated by flow cytometer (FACS Canto™ II, BD BioSciences, San Jose, CA, USA) equipped with a 488 nm laser.

2.4.2. Transmission electron microscopy

Approximately 5×10^5 cells were treated with ZnO NPs (20 μg/mL) for 6 h; thereafter the cells were centrifuged at 376 g for 5 min. The pellet formed was resuspended in sodium cacodylate buffer (0.1 M, 200 μL), and fixed in 2.5% glutaraldehyde overnight at 4 °C. The pellet was post fixed in osmium tetroxide for 1.5 h at 4 °C in dark. Further, the pellet was dehydrated in increasing percentage of acetone, ethanol and embedded in epoxy resin. The sample was then cut into thin sections by diamond knife ultramicrotome and mounted on copper grids. Observations were carried by TEM (Technai™ G2 Spirit, FEI Company, The Netherlands) at an accelerating voltage of 80 kV.

2.5. Cytotoxicity assays

2.5.1. MTT assay

Cell viability of ZnO NP treated cells was determined by MTT assay according to the method of Mosmann (1983). Briefly, THP-1 cells were seeded in PLL coated plates for 24 h, exposed to ZnO NPs for 3, 6 and 24 h. PLL is a polycation which enhances electrostatic interaction between negatively charged ions of THP-1 cell membrane and the culture surface to adhere THP-1 cells to the surface of the plate. After exposure, treatment was removed and cells were incubated with MTT (3-(4,5- dimethythiazoyl-2-yl)-2,5-diphenyltetrazolium bromide) dye for 3 h. Thereafter, formazan crystals were solubilised by dimethysulphoxide and measured

spectrophotometrically at 530 nm in a plate reader (SYNERGY-HT multiwell plate reader, Bio-Tek, Winooski, VT, USA) using KC4 software. A parallel set of experiment without cells were conducted to check the interference of ZnO NPs with MTT dye.

2.5.2. LDH activity

Lactate dehydrogenase (LDH) release was determined by LDH assay kit (Sigma Chemical Co. Ltd., St Louis, MO, USA) using manufacturer's protocol. The absorbance of resulting coloured formazan was measured at 490 and 690 nm in a plate reader (SYNERGY-HT multiwell plate reader, Bio-Tek, Winooski, VT, USA) using KC4 software. A parallel set of experiment without cells were conducted to check the interference of ZnO NPs with dye.

2.6. Oxidative and nitrosative stress markers

2.6.1. ROS generation

ROS generation was determined using 2, 7-dichlorofluorescein diacetate (DCFDA; Sigma Chemical Co. Ltd., St Louis, MO, USA). Cells (1×10^5 cells per well) were treated with different concentrations (0.5, 1, 5, 10, 15 and 20 μg/mL) of ZnO NPs for 6 h. After exposure, cells were centrifuged and pellet was washed with 1 x PBS and resuspended in 20 μM of DCFDA prepared in 1 x PBS. Cells were then incubated for 20 min at 37 °C and fluorescence intensity was detected by flow cytometer (FACS Canto™ II, BD BioSciences, San Jose, CA, USA) equipped with a 488 nm laser.

2.6.2. Glutathione (GSH) estimation

Free sulphydryl content was measured as described by Ellman (1959). Briefly, cells were exposed to different concentrations (0.5, 1, 5, 10, 15 and 20 μg/mL) of ZnO NPs for 6 h. Thereafter, the cells were sonicated in 0.5 mL of 1 x PBS. To 0.5 mL of homogenate, 0.5 mL of 5% tri-chloro acetic acid (TCA) was added and centrifuged at 845 g for 15 min at 4 °C. Further, 0.5 mL of the supernatant was added to 2.5 mL of 0.01% 5,5′-dithiobis(2-nitrobenzoic acid) (DTNB) and the absorbance was read at 412 nm. The protein present in the pellet was determined by the Bradford method (Bradford, 1976) and the concentration of GSH was expressed as μmol/mg protein.

2.6.3. Nitric oxide determination

Nitric oxide was estimated in cell culture medium as stable nitrite using Greiss reagent as described by Green et al. (1982). 10,000 cells were treated with varying concentrations of ZnO NPs for 6 h in PLL coated 96 well plates as PLL enhances the adherence of THP-1 cells to the culture surface. It is based on the azo dye formation from diazonium salt (formed from reaction between sulfanilic acid and nitrite) coupling to naphthylethylenediamine dihydrochloride. The absorbance was read at 540 nm and nitric oxide concentration was determined using sodium nitrite as the standard.

2.7. Cytokines quantitation

5×10^5 Cells per well in a 24 well plate were exposed to ZnO NPs for 3 h. Thereafter, the supernatant was stored at −80 °C. The release of cytokines in the supernatant was quantitated using BD™ cytometric bead array (CBA) human Th-1/Th-2 Cytokine Kit II according to the manufacturer's protocol (BD Biosciences, San Jose, CA, USA). 50 μL of samples were incubated with 50 μL of mixed capture antibodies along with 50 μL of Phycoerythin detection reagent to form sandwich complexes. Samples were evaluated by flow cytometer (FACSCanto™ II, BD BioSciences, San Jose, CA, USA) and the results were analysed using FCAP Array™ software.

2.8. Western blot analysis

For western blot analysis, control and 6 h ZnO NP treated cells were pelleted and lysed using CelLytic™ M Cell Lysis Reagent (Sigma Chemical Co. Ltd. St. Louis, MO, USA) in the presence of Na-orthovanadate, Na-fluoride and protease inhibitor cocktail. Protein isolated, was estimated by Bradford method (Bradford, 1976) and bovine serum albumin (BSA) was used as standard. Thirty micrograms of total protein was resolved in 10% and 12% SDS polyacrylamide gel electrophoresis at 25 mA/40 V. When the loading dye reaches the bottom of the gel, the power is turned off. The proteins are then electrotransferred at 300 mA/100 V for 3 h onto polyvinylidene fluoride membranes. The blotted membrane was blocked with 5% non-fat dry milk and 2% BSA in PBS containing 0.1% Tween 20 (blocking solution), and incubated with specific antibodies against rabbit-monoclonal to nuclear factor kappa B (NF-κB Product no. #3033; 1:1000), rabbit-monoclonal to p-ERK1/2 (Product no. #4376; 1:1000), rabbit-monoclonal to p-p38 (Product no. #4631: 1:1000), mouse-monoclonal to p-JNK (Product no. #9255; 1:1000), rabbit-polyclonal to ERK1/2 (Product no. #9102; 1:1000), rabbit-polyclonal to p38 (Product no. #9212; 1:1000), rabbit-polyclonal to JNK (Product no. #9252; 1:1000), mouse-monoclonal to IL-1β (Product no. #12242; 1:500) and rabbit-polyclonal to COX-2 (Product no. #4842; 1:1000) purchased from Cell Signaling Technology (Danvers, MA, USA). The blots were further incubated with horse radish peroxidase conjugated secondary antibody (1:5000, anti-rabbit polyclonal IgG SAB 3700941 and anti-mouse polyclonal IgG SAB 3701116; Sigma Chemical Co. Ltd., St. Louis, MO, USA) and developed in gel doc (Syngene Bioimaging Private Ltd., Gurgaon, Haryana, India) by enhanced chemiluminescence (Super Signal West Femto Chemiluminescent reagent, Pierce, Rockford, IL, USA). All the blots were stripped and reprobed with rabbit-polyclonal to β-actin (Product no. #4967; 1:10000) to ensure equal loading of protein. Quantification of the western blots intensity was done by Image J software (NIH, USA).

2.9. Genotoxicity assessment

2.9.1. Comet assay

THP-1 cells (75000 cells per well) were exposed to ZnO NPs for 3 h. Cells were harvested and slides were prepared according to the method described by Singh et al. (1988) and modified by Bajpayee et al. (2005). Cells were lysed in chilled lysing solution (2.5 M NaCl, 100 mM EDTA, 10 mM trizma base (pH 10), along with 1% triton X-100 added just before use) and kept overnight at 4 °C. Electrophoresis was performed at 24 V (~0.74 V/cm) and 300 mA for 30 min, neutralized with tris buffer (0.4 M, (pH − 7.5)) and stained with 80 μL of 20 μg/mL EtBr. The study design was as follow; Group 1 − control; Group 2 − positive control; Group 3 to Group 8− ZnO NPs (0.5, 1, 5, 10, 15 and 20 μg/mL). 50 random cells (25 cells from each replicate slide) were analysed for each group as per the guidelines (Tice et al., 2000) at 400× magnification and DNA fragmentation was analysed by using an image analysis system (Komet 4.0, ANDOR technology, Belfast, UK.). 16 slides per experiment was analysed and the experiment was performed in triplicate, therefore a total of 48 (16X3) slides were scored.. The % tail DNA and Olive tail moment (OTM; product of tail length and the fraction of total DNA in the tail) (Olive et al., 1993) was analysed.

2.9.2. Cytokinesis-block micronucleus (CBMN) assay

CBMN assay was carried according to the method of Fenech (2000). Cells were treated with ZnO NPs for 3 h, centrifuged, washed with 1 x PBS and suspended in complete medium containing cytochalasin-B at a final concentration of 3 μg/mL, in an incubator for 23 h. The cells were harvested and slides for each

Table 1
Characterization of ZnO NPs by TEM, SEM and DLS.

Nanoparticle	TEM size	SEM size	DLS (hydrodynamic diameter in Milli-Q water)	DLS (hydrodynamic diameter in media)	Zeta potential in Milli-Q water	Zeta potential in media
ZnO	~30 nm	~30 nm	297 nm	264.4 nm	−25.3 mV	−13.4 mV

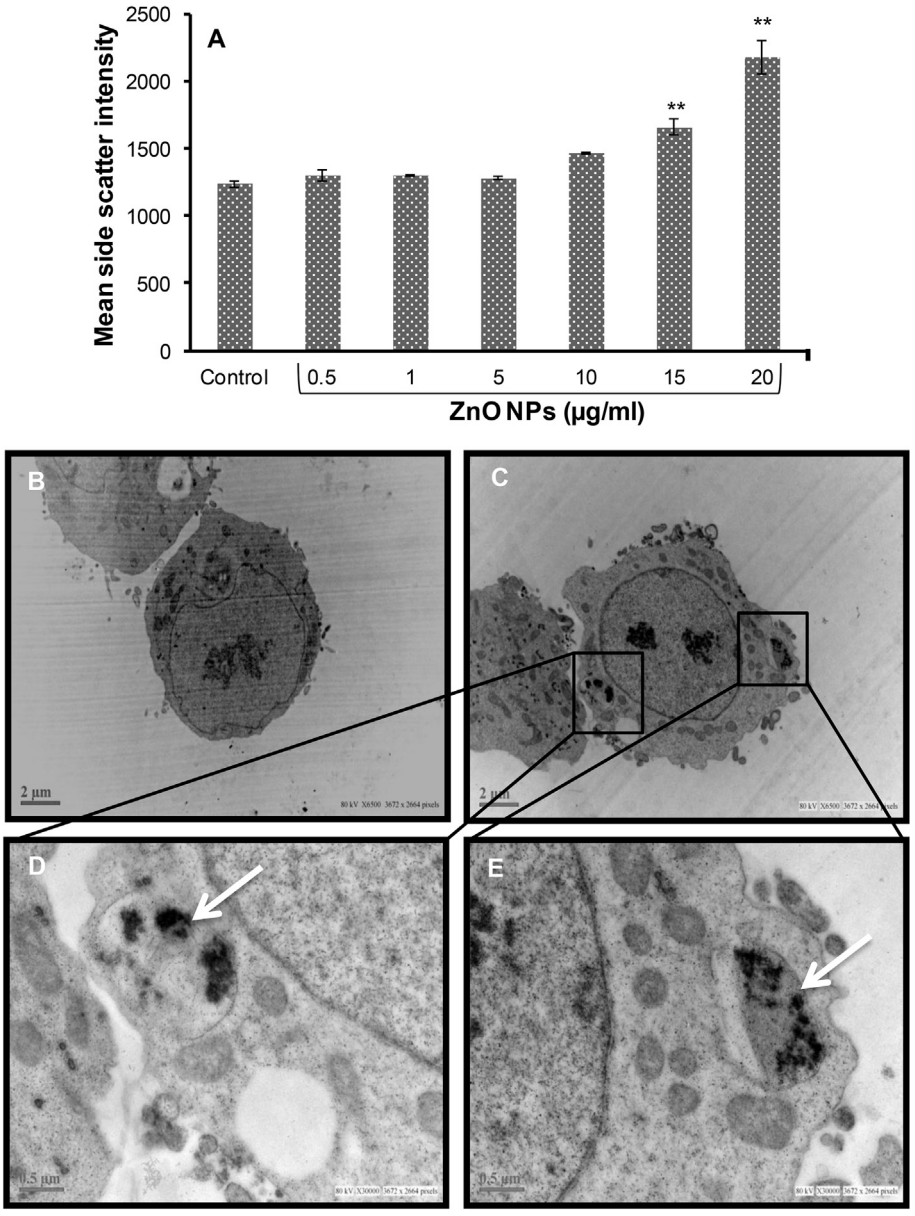

Fig. 1. Internalization of ZnO NPs in THP-1 cells. (A) Analysis of internalization of ZnO NPs by flow cytometric parameter viz. SSC intensity (B) Control cells, (C) ZnO NPs treated cells and (D–E) are higher magnification of area marked with black boxes in (C); white arrows indicate accumulation of NPs inside endosomes.

concentration were prepared by centrifuging cells using the cytospin (Thermo Shandon, Hampshire, UK). Two thousand binucleate cells from each concentration (1000 binucleate cells from each slide, 500 cells per dot) were scored. Total of 16 slides in each experiment was analyzed and experiment was performed thrice. The slides were fixed in chilled methanol for 5 min, air dried and stored until staining. The slides were stained with 20 µg/mL acridine orange and observed for the presence of micronuclei (MN) in 2000 binucleated cells (BNCs) using fluorescent microscope (DMLB, Leica, Wetzlar, Germany) at 400× magnification. The presence of micronucleus (MN) in 2000 BNCs was counted and the result for the MN frequency was expressed as MN/1000 BNCs.

The nuclear division index (NDI) was also calculated from 500 cells per concentration according to the formula:

NDI = (No. of mononucleate cells +2 x No. of binucleate cells +3 x No. of trinucleate cells +4 x No. of quadrinuclear cells)/Total No. of cells.

2.10. Statistical analysis

Results were expressed as mean ± standard error of mean (S.E.M.) of three experiments and data were analyzed using one

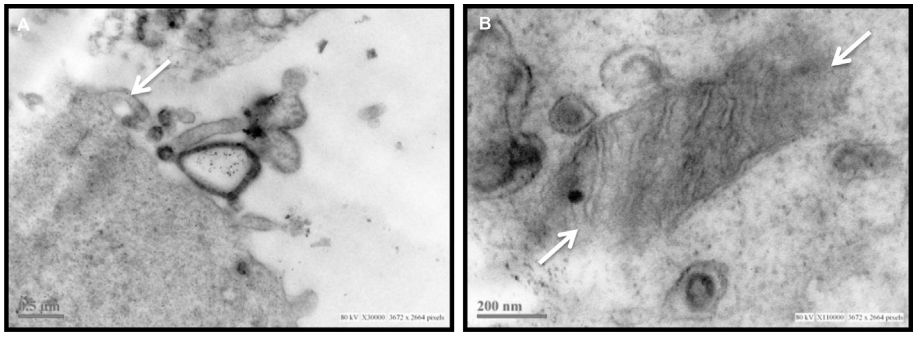

Fig. 2. TEM photomicrographs showing ultrastructural changes in ZnO NP treated cells. The white arrows indicate (A) endosome formation and (B) mitochondrial membrane disintegration.

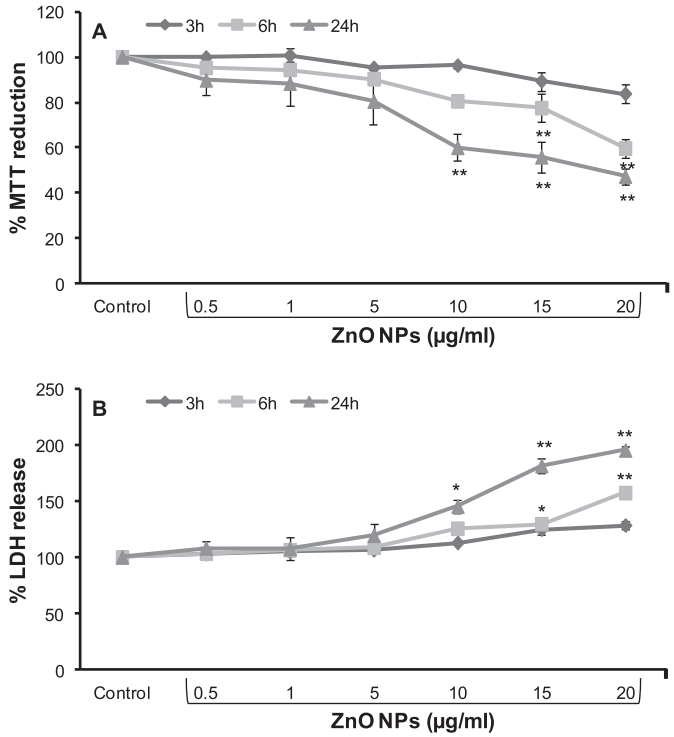

Fig. 3. Concentration and time dependent cytotoxicity of ZnO NPs in THP-1 cells, (A) % MTT reduction, (B) % LDH release. Results represent mean ± S.E.M. of three independent experiments. *$p < 0.05$, **$p < 0.01$, when compared to control.

way analysis of variance (ANOVA) followed by a Dunnett's post hoc multiple comparison test from GraphPad Prism-3.0 (GraphPad Prism software, San Diego, California, USA). In all cases, $p < 0.05$ and $p < 0.01$ was considered significant.

3. Results

3.1. Particle characterization

ZnO NPs was in the form of white solid nanopowder. The specific surface area was 15–25 m^2/g (as described in the product specification sheet obtained from Sigma Chemical Co. Ltd., St. Louis, MO, USA). The mean hydrodynamic size of ZnO NPs as determined by DLS is 264.4 nm in RPMI medium and 297 nm in Milli-Q water. The zeta potential in RPMI medium is −13.4 mV and in Milli-Q water is −25.3 mV. The average size of ZnO NPs measured by TEM and SEM was 30 nm (Table 1).

3.2. Cellular uptake of ZnO NPs

A significant ($p < 0.01$) concentration dependent increase in SSC intensity was observed (Fig. 1A) in ZnO NP treated cells indicating their internalization. At exposure concentration 15 and 20 µg/mL the mean SSC intensity (arbitrary unit) was 1662 and 2182.6 respectively, as compared to the control (1242). Internalization of the NPs in cells was also observed in TEM, where ZnO NPs were found to be localised in the endosomes (Fig. 1C–E) as compared to control (Fig. 1B). A distinct endosome formation as well as disintegration of the mitochondrial membrane was observed in ZnO NP treated cells (Fig. 2A–B).

3.3. Cytotoxicity assessment

MTT and LDH assays demonstrated a significant ($p < 0.05$, $p < 0.01$) concentration and time dependent increase in the cytotoxicity in THP-1 cells after ZnO NPs exposure.

The mitochondrial succinate dehydrogenase activity was reduced to 83.8%, 59.7% and 47.4% respectively after 3, 6 and 24 h of exposure to 20 µg/mL ZnO NPs in THP-1 cells, as compared to control (Fig. 3A).

A significant ($p < 0.05$, $p < 0.01$) increase (181.2% and 195.1%) in LDH release was observed in cells treated with 15 and 20 µg/mL ZnO NPs after 24 h (Fig. 3B).

3.4. Evaluation of oxidative stress

ZnO NPs (15 and 20 µg/mL) treated cells showed a significant ($p < 0.05$) concentration dependent increase in the intracellular ROS as observed by the increase in the intensity of fluorescence of DCFDA dye (Fig. 4A). A significant ($p < 0.05$) concentration dependent reduction in GSH levels (65.6% and 61.2%) was observed in cells treated with ZnO NPs (15 and 20 µg/mL) for 6 h (Fig. 4B). Also, a concentration dependent significant ($p < 0.05$) increase in nitrite levels was observed in cells treated with ZnO NPs (15 and 20 µg/mL) when compared to control (Fig. 4C).

3.5. Cytokine quantitation

A statistically significant ($p < 0.01$) increase in the level of tumour necrosis factor-alpha (TNF-α; Fig. 5) was observed in cells treated with ZnO NPs at concentrations ranging from 5 to 20 µg/mL. Release of IL-6 and INF-γ was also obtained but the results were not significant compared to control (data not shown).

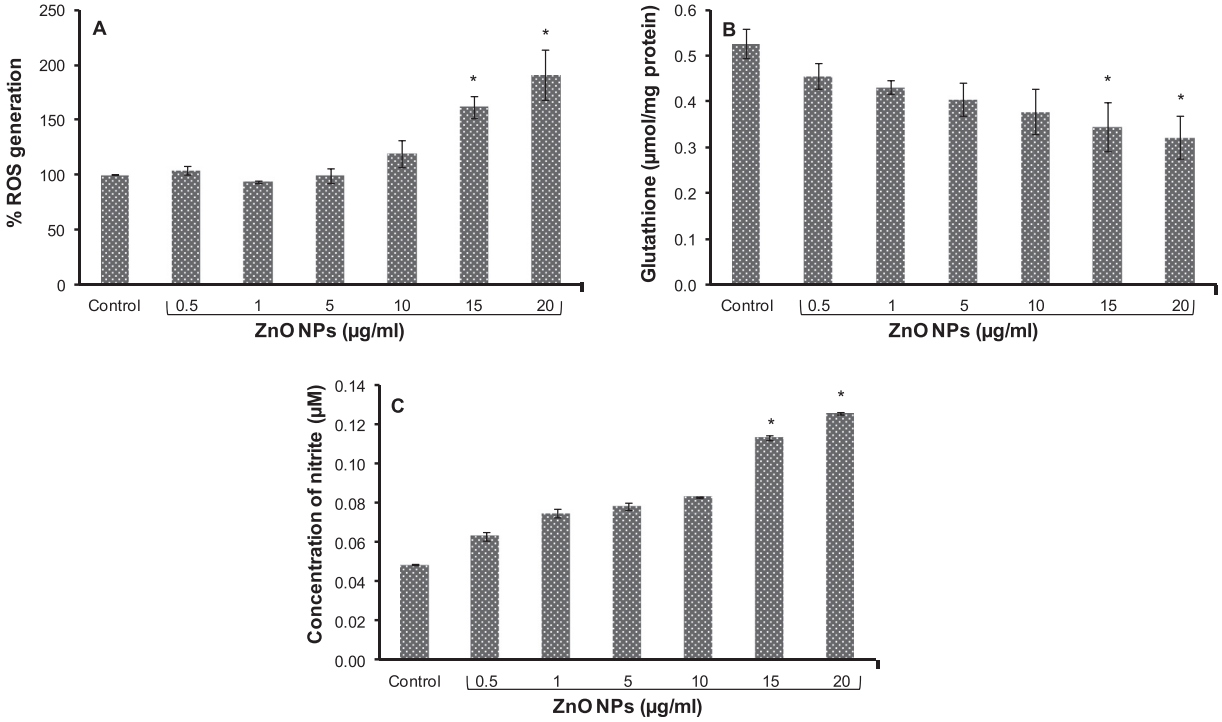

Fig. 4. Effect of ZnO NPs on, (A) Reactive oxygen species (ROS), (B) Glutathione (GSH) and (C) Nitrite levels. Data represents the mean ± S.E.M. of three independent experiments. *p < 0.05 when compared with control.

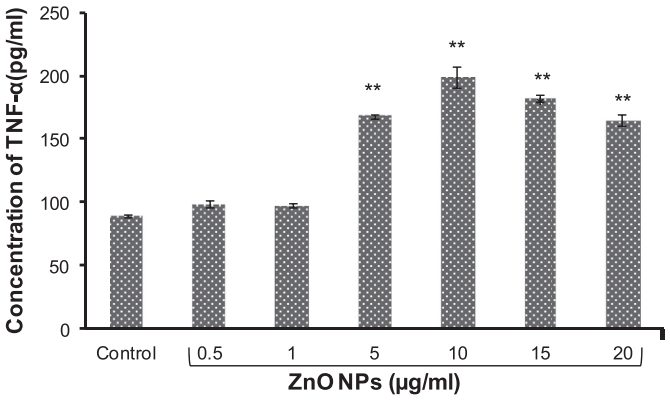

Fig. 5. Effect of ZnO NPs on TNF-α release in THP-1 cells. Data represents the mean ± S.E.M. of three independent experiments. **p < 0.01 when compared with control.

3.6. Western blot analysis

A significant ($p < 0.05$, $p < 0.01$) increase (1.9–2.6 fold) in the levels of inflammatory marker proteins (IL-1β, COX-2) and transcription factor (NF-κB) in THP-1 cells was observed after treatment with ZnO NPs (20 µg/mL; Fig. 6A and C).

Also, a significant ($p < 0.05$, $p < 0.01$) increase (1.67–2.25 fold) in phosphorylation of proteins viz extracellular signal-regulating kinase (ERK1/2), Jun-N-terminal kinase (JNK) and p38 was observed in cells treated with 20 µg/mL ZnO NPs. However, no significant change was observed in the expression levels of total ERK1/2, JNK and p38 which also confirmed equal protein loading. The expression profile of β actin was used as an internal control for protein loading in control and ZnO NPs treated samples (Fig. 6B and D).

3.7. Genotoxic potential of ZnO NPs

Comet assay data showed a significant ($p < 0.05$) increase in DNA damage as evident from the Olive tail moment (OTM) and tail DNA (%) values. The cells treated with ZnO NPs (20 µg/mL) exhibited an OTM of 3.11 in comparison to control (0.84; Table 2).

Increase in number of micronucleated cells was also observed with increasing concentration of ZnO NPs (10, 15 and 20 µg/mL) when compared to control. At the highest concentration of ZnO NPs (20 µg/mL) a significant ($p < 0.01$) increase in the micronucleus frequency (20.67 MN/1000 BNCs) was observed as compared to the control (7.33 MN/1000 BNCs; Table 3).

4. Discussion

Monocytes play a significant role in the host defence against any foreign body including microorganisms. Therefore, in the present study it was thought prudent to use monocytes as a model to investigate the immunotoxicity of ZnO NPs. The innate immune mechanism detects the nonself antigens, resulting in imbalance of pro-inflammatory and cell signalling molecules. Therefore, the evaluation of pro-inflammatory response in monocytes treated with ZnO NPs is important in nanotoxicological assessments.

Exposure of ZnO NPs elicits cytotoxic, genotoxic and pro-inflammatory responses (Hackenberg et al., 2011; Sharma et al., 2009). Prach et al. (2013) demonstrated that ZnO NPs exposure to THP-1 cells did not induce the release of pro-inflammatory cytokines. This was due to the fact that the cytokine got bound to ZnO NPs after 24 h of incubation and was masked from being detected in the ELISA. To overcome the shortcomings, the present study was designed to evaluate the immunomodulatory effect of ZnO NPs in THP-1 cells after 3 h and the mechanism of inflammatory response was also determined.

Size of the NPs is a crucial parameter that determines their

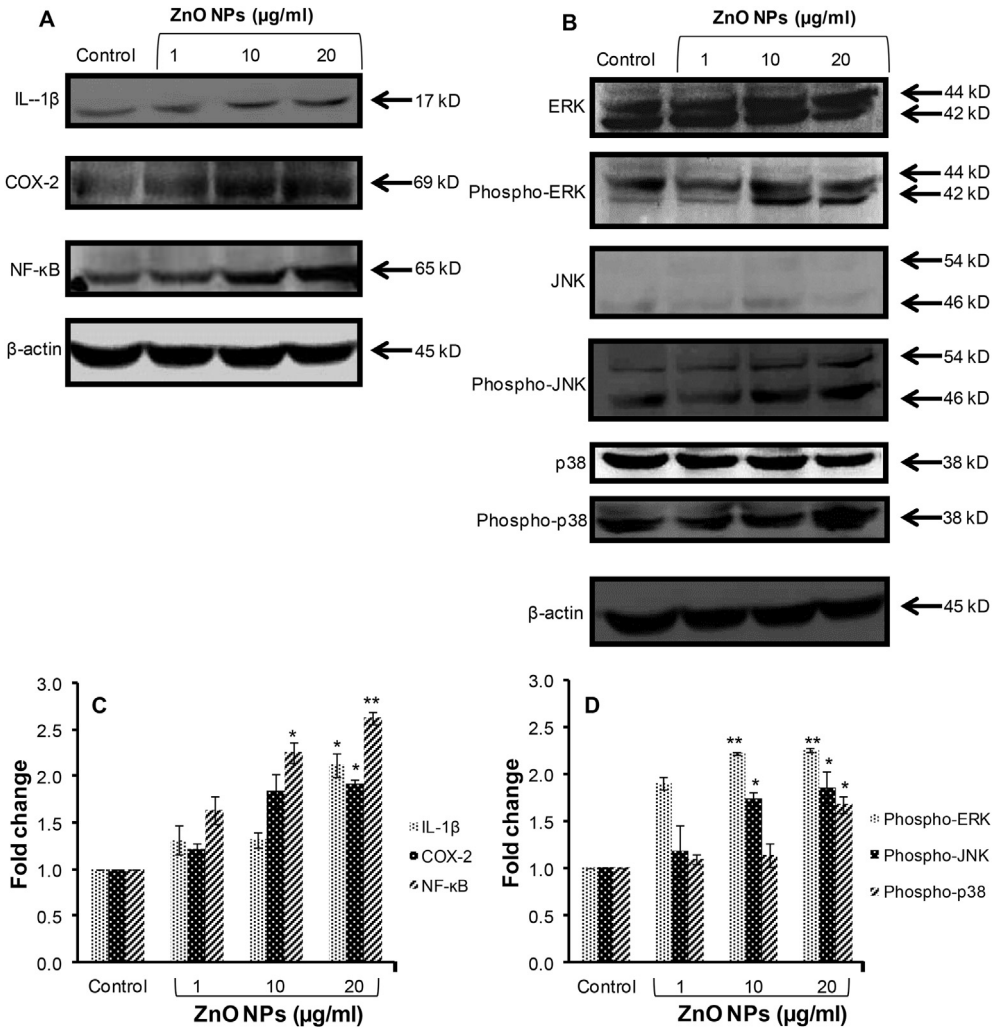

Fig. 6. Western blot analysis of proteins from THP-1 cells treated with ZnO NPs (1, 10 and 20 μg/mL). (A) IL-1β, COX-2 and NF-κB, (B) MAPK signalling proteins (phospho- ERK1/2, phospho-JNK and phospho-p38) and the corresponding (C and D) bar graphs showing their densitometric analysis. β-actin was used as internal control. Results represent mean ± S.E.M. of three independent experiments. *p < 0.05, **p < 0.01, when compared to control.

Table 2
DNA damage in THP-1 cells after 3 h exposure to ZnO NPs as evident by Comet parameters.

Groups	OTM[a] (arbitrary unit)	Tail DNA (%)
Control	0.84 ± 0.08	7.92 ± 0.60
1 mM EMS[b]	19.00 ± 0.53**	64.75 ± 0.90**
ZnO NPs (0.5 μg/mL)	1.83 ± 0.46	15.86 ± 2.27*
ZnO NPs (1 μg/mL)	2.13 ± 0.43	18.63 ± 2.08**
ZnO NPs (5 μg/mL)	2.46 ± 0.46	20.67 ± 1.56**
ZnO NPs (10 μg/mL)	2.58 ± 0.49	21.54 ± 1.97**
ZnO NPs (15 μg/mL)	2.69 ± 0.48	21.87 ± 2.04**
ZnO NPs (20 μg/mL)	3.11 ± 0.85*	23.59 ± 3.59**

Values are expressed as mean ± S.E.M. of three experiments.
*p < 0.05, **p < 0.01 when compared with control.
[a] OTM-Olive tail moment.
[b] EMS-ethyl methanesulphonate-positive control.

potential to induce cytokine production; hence, the particle needs to be characterized thoroughly in suspension and powder form (Zolnik et al., 2010). In the present study, the size of ZnO NPs as measured by DLS in complete RPMI media and Milli-Q water was 264.4 and 299 nm respectively. The decrease in size of NPs in media has been attributed to the presence of serum which coats the particles and thus decreases agglomeration (Dhawan and Sharma, 2010; Kumar et al., 2011b).

Since these NPs fall within a small size distribution range, they can easily enter into the cells and localise in the organelles. The present study, through TEM measurements clearly shows that ZnO NPs enter the cells through endocytosis or phagocytosis as evidenced by the formation of endosomes (Fig. 2A). The internalization was further confirmed by the flow cytometry data where a concentration-dependent increase in the intensity of SSC was observed. It has been shown that SSC intensity is an indicator for the uptake of NPs (Kumar and Dhawan, 2013; Kumar et al., 2011a; Shukla et al., 2013; Suzuki et al., 2007). Distribution of these NPs inside cells would therefore enable their interactions with biological macromolecules, including lipids, proteins and nucleic acids thereby eliciting toxic responses.

In the present study, THP-1 cells were exposed to ZnO NPs at different concentrations (0.5, 1, 5, 10, 15 and 20 μg/mL) and time points (3, 6 and 24 h). The endocytosed particles showed significant cytotoxicity at concentration 10, 15 and 20 μg/mL after 6 and 24 h of exposure as observed in MTT and LDH release assay. However, the cells were more than 80% viable after 3 h exposure of ZnO NPs. Hence, this time point was used for the immunomodulatory and genotoxicity studies.

Table 3
Effect of ZnO NPs on micronucleus formation in THP-1 cells.

Groups	No. of MN/1000 BNCs	NDI[a]	% BNCs/500 viable cells
Control	7.33 ± 0.33	1.99 ± 0.002	100 ± 0.00
1 mM EMS[b]	24.67 ± 0.33**	1.82 ± 0.001**	82.90 ± 0.36**
ZnO NPs (0.5 μg/mL)	7.67 ± 0.67	1.98 ± 0.003	99.12 ± 0.18
ZnO NPs (1 μg/mL)	8.67 ± 1.45	1.98 ± 0.002	98.38 ± 0.12**
ZnO NPs (5 μg/mL)	11.67 ± 1.45	1.96 ± 0.003**	95.89 ± 0.24**
ZnO NPs (10 μg/mL)	15.00 ± 1.53**	1.96 ± 0.005**	93.60 ± 0.24**
ZnO NPs (15 μg/mL)	17.67 ± 1.45**	1.95 ± 0.005**	93.27 ± 0.35**
ZnO NPs (20 μg/mL)	20.67 ± 0.67**	1.91 ± 0.005**	89.16 ± 0.36**

Values are expressed as mean ± S.E.M. of three experiments.
*p < 0.05, **p < 0.01 when compared with control.
[a] NDI- Nuclear division index.
[b] EMS- ethyl methane sulphonate-positive control.

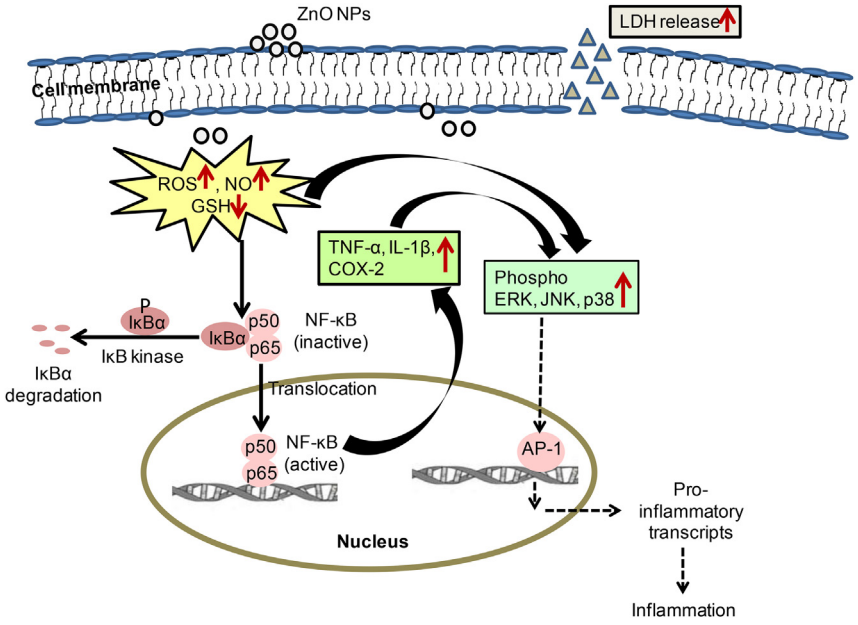

Fig. 7. A schematic showing possible mechanism of ZnO NPs induced inflammatory response in human monocytic cells. The dotted lines represent the pathway of other inflammatory mediators activated during inflammation. Activator protein 1 (AP-1).

The entry of ZnO NPs into the cells induced mitochondrial membrane damage as observed in TEM (Fig. 2B). This led to ROS generation, oxidative stress and inflammatory response. This is in accordance with similar studies reported earlier (Sharma et al., 2009, 2011; Xia et al., 2008) which show that such responses lead to protein, membrane and DNA damage. Our data showed a significant increase in ROS generation and depletion in GSH levels with a concomitant increase in nitrite production revealing that ZnO NPs induce oxidative and nitrosative stress. The semiconductor property of ZnO NPs is also considered as one of the probable reason for ROS generation. Crystalline ZnO NPs have a band gap of ~3.3 eV (Lany et al., 2007). Due to transfer of electrons from valence band to conduction band, electron holes are created in the valence band. Electrons and holes sometimes reach the surface of NPs where, electrons react with oxygen and holes react with hydroxyl ions or water forming superoxide and hydroxyl radicals. As the size of ZnO NPs decreases, crystal defects are created, forming a large number of electron–hole pairs. The holes act as oxidants and can split water molecules into H^+ and OH^- while the conduction band electrons act as reducers and reacts with dissolved oxygen molecules to generate superoxide radical anions (Rasmussen et al., 2010). NO and ROS are known to cooperatively act in the *in vivo* vasodilation of endothelium walls thus leading to the release of pro-inflammatory mediators (Kvietys and Granger, 2012).

Our study also showed that ZnO NPs stimulated the release of pro-inflammatory cytokines, IL-1β and TNF-α. These results are consistent with the data reported earlier on nasal mucosa cells (Hackenberg et al., 2011). Increase in expression of inflammatory marker, COX-2 was obtained on ZnO NPs treatment in cells. The oxidative and nitrosative stress response upregulates the expression of the inflammatory mediators such as IL-1β, TNF-α and COX-2 via the activation of the transcription factor NF-κB (Lu and Wahl, 2005). NF-κB gets activated by the phosphorylation of inhibitory protein (IκBα) by IκB Kinase and concomitant translocation of NF-κB (p50, p65) from cytoplasm to nucleus. A significant concentration dependent increase in the expression of NF-κB was obtained, which is a pivotal mediator involved in multiple cellular responses and regulates the release of pro-inflammatory mediators (Bonizzi and Karin, 2004). Therefore, the activation of NF-κB explains the enhanced expression of inflammatory cytokines.

The present study showed that ZnO NPs cause DNA damage as evident from the data of the Comet and CBMN assays. This could be attributed to the uptake of NPs as evident by TEM in conjunction with an increase in ROS and nitrite levels along with decrease in GSH (AshaRani et al., 2009; Kumar and Dhawan, 2013; Sharma et al., 2012, 2011). The release of inflammatory cytokines could

also be a probable reason for DNA damage caused by ZnO NPs (Totsuka et al., 2014).

Additionally, the role of signalling pathways involved in inflammatory response was explored. In the present study, it was observed that the JNK, ERK1/2 and p38 that constitute the MAPK cascade play a key role in the inflammatory response of ZnO NPs as evident from the increased expression levels of phosphorylated JNK, phosphorylated ERK1/2 and phosphorylated p38. The increase in oxidative and nitrosative stress induced the activation of MAPK proteins (Kumar et al., 2015; Mccubrey et al., 2006). MAPKs phosphorylate specific serine, threonine and tyrosine residues of these proteins thereby modulating their function. Studies have shown that JNK, a major subgroup of MAPK, is activated primarily by inflammatory cytokines and environmental stress and phosphorylated on threonine-183 and tyrosine-185 residues by the dual specific kinases MKK4 and MKK7 (Davis, 2000). p38 is phosphorylated by MKK3 on threonine-180 and tyrosine-182 and MAPK/ERK kinases (MEK1 and MEK2) phosphorylate ERK1/2 within a conserved threonine-glutamine-tyrosine motif (Raingeaud et al., 1995; Roux and Blenis, 2004). Activation of both ERK1/2 and p38 kinase is necessary in cytokine gene expression (Carter et al., 1999). Therefore, corroborating with the earlier studies our results demonstrate that ZnO NPs induced inflammatory cytokines mediated the activation of MAPK proteins. The phosphorylation of JNK, ERK1/2 and p38 could further activate the transcription factor, activator protein 1 (AP-1), consequently leading to enhanced pro-inflammatory transcripts causing inflammation.

In conclusion, our study determined the immunomodulatory effect of ZnO NPs and led to the determination of the possible pathway of ZnO NPs induced inflammatory response as depicted in Fig. 7. Therefore the indiscriminate use of NPs in cosmetics, paints and other consumer goods should be avoided and guidelines should be implemented for NPs usage.

Acknowledgements

This work was supported by the Council of Scientific and Industrial Research, New Delhi, India through network projects NWP35 and NanoSHE (BSC0112), and the EU Framework Programme (FP7/2007-2013) under Grant Agreement 263147 (NanoValid- Development of reference methods for hazard identification, risk assessment and LCA of engineered nanomaterials) is acknowledged. The funding received from the Gujarat Institute of Chemical Technology, India under CENTRA (Centre for Nanotechnology and Research Application) project in grant agreement number (ILS/GICT/2013/003) is also gratefully acknowledged. Violet A. Senapati thanks Council of Scientific and Industrial Research (CSIR), New Delhi for the award of Junior and Senior Research Fellowship.

Transparency document

Transparency document related to this article can be found online at http://dx.doi.org/10.1016/j.fct.2015.06.018.

References

AshaRani, P.V., Low, K.M.G., Hande, M.P., Valiyaveettil, S., 2009. Cytotoxicity and genotoxicity of silver nanoparticles in human cells. ACS Nano 3, 279–290.
Bajpayee, M., Pandey, A.K., Parmar, D., Mathur, N., Seth, P.K., Dhawan, A., 2005. Comet assay responses in human lymphocytes are not influenced by the menstrual cycle: a study in healthy Indian females. Mutat. Res. 565, 163–172.
Bonizzi, G., Karin, M., 2004. The two NF-kappa B activation pathways and their role in innate and adaptive immunity. Trends Immunol. 25, 280–288.
Bradford, M.M., 1976. A rapid and sensitive method for the quantitation of microgram quantities of protein utilizing the principle of protein-dye binding. Anal. Biochem. 72, 248–254.
Carter, A.B., M, M.M., Hunninghake, G.W., 1999. Both Erk and p38 kinases are necessary for cytokine gene transcription. Am. J. Respir. Cell Mol. Biol. 20, 751–758.
Davis, R.J., 2000. Signal transduction by the JNK group of MAP kinases. Cell 103, 239–252.
Dhawan, A., Sharma, V., 2010. Toxicity assessment of nanomaterials: methods and challenges. Anal. Bioanal. Chem. 398, 589–605.
Dobrovolskaia, M.A., Aggarwal, P., Hall, J.B., McNeil, S.E., 2008. Preclinical studies to understand nanoparticle interaction with the immune system and its potential effects on nanoparticle biodistribution. Mol. Pharm. 5, 487–495.
Ekwall, B., Silano, V., Paganuzzi-Stammati, A., Zucco, F., 1990. In: Bourdeau, P., et al. (Eds.), Chapter 7- Toxicity Tests with Mammalian Cell Cultures. Short-term Toxicity Tests for Non-genotoxic Effects. John Wiley & Sons, Inc, New York, pp. 75–97.
Ellman, G.L., 1959. Tissue sufhydryl groups. Arch. Biochem. Biophys. 82, 70–77.
Fenech, M., 2000. The *in vitro* micronucleus technique. Mutat. Res. 455, 81–95.
Fortina, P., Kricka, L.J., Graves, D.J., Park, J., Hyslop, T., Tam, F., Halas, N., Surrey, S., Waldman, S.A., 2007. Applications of nanoparticles to diagnostics and therapeutics in colorectal cancer. Trends Biotechnol. 25, 145–152.
Green, L.C., Wagner, D.A., Glogowski, J., Skipper, P.L., Wishnok, J.S., Tannenbaum, S.R., 1982. Analysis of nitrate, nitrite, and [15N] nitrate in biological samples. Anal. Biochem. 126, 131–138.
Hackenberg, S., Scherzed, A., Technau, A., Kessler, M., Froelich, K., Ginzkey, C., Koehler, C., Burghartz, M., Hagen, R., Kleinsasser, N., 2011. Cytotoxic, genotoxic and pro-inflammatory effects of zinc oxide nanoparticles in human nasal mucosa cells in vitro. Toxicol. Vitro 25, 657–663.
Hanley, C., Layne, J., Punnoose, A., Reddy, K.M., Coombs, I., Coombs, A., Feris, K., Wingett, D., 2008. Preferential killing of cancer cells and activated human T cells using ZnO nanoparticles. Nanotechnology 19, 295103.
Hong, T.K., Tripathy, N., Son, H.J., Ha, K.T., Jeong, H.S., Hahn, Y.B., 2013. A comprehensive in vitro and in vivo study of ZnO nanoparticles toxicity. J. Mater. Chem. B 1, 2985–2992.
Johnston, H.J., Hutchison, G., Christensen, F.M., Peters, S., Hankin, S., Stone, V., 2010. A review of the in vivo and in vitro toxicity of silver and gold particulates: particle attributes and biological mechanisms responsible for the observed toxicity. Crit. Rev. Toxicol. 40, 328–346.
Kreuter, J., Gelperina, S., 2008. Use of nanoparticles for cerebral cancer. Tumori 94, 271–277.
Kumar, A., Dhawan, A., 2013. Genotoxic and carcinogenic potential of engineered nanoparticles: an update. Arch. Toxicol. 87, 1883–1900.
Kumar, A., Khan, S., Dhawan, A., 2014. Comprehensive molecular analysis of the responses induced by titanium dioxide nanoparticles in human keratinocyte cells. J. Transl. Toxicol. 1, 28–39.
Kumar, A., Najafzadeh, M., Jacob, B.K., Dhawan, A., Anderson, D., 2015. Zinc oxide nanoparticles affect the expression of p53, Ras p21 and JNKs: an ex vivo/in vitro exposure study in respiratory disease patients. Mutagenesis 30, 237–245.
Kumar, A., Pandey, A.K., Singh, S.S., Shanker, R., Dhawan, A., 2011a. A flow cytometric method to assess nanoparticle uptake in bacteria. Cytom. Part A 79A, 707–712.
Kumar, A., Pandey, A.K., Singh, S.S., Shanker, R., Dhawan, A., 2011b. Engineered ZnO and TiO2 nanoparticles induce oxidative stress and DNA damage leading to reduced viability of *Escherichia coli*. Free Radic. Biol. Med. 51, 1872–1881.
Kvietys, P.R., Granger, D.N., 2012. Role of reactive oxygen and nitrogen species in the vascular responses to inflammation. Free Radic. Biol. Med. 52, 556–592.
Lany, S., Osorio-Guillen, J., Zunger, A., 2007. Origins of the doping asymmetry in oxides: hole doping in NiO versus electron doping in ZnO. Phys. Rev. B 75, 2031–2034.
Lu, Y., Wahl, L.M., 2005. Oxidative stress augments the production of matrixmetalloproteinase-1, cyclooxygenase-2, and prostaglandin E2 through enhancement of NF-Kappa B activity in lipopolysaccharide-activated human primary monocytes. J. Immunol. 175, 5423–5429.
Mccubrey, J.A., Lahair, M.M., Franklin, R.A., 2006. Reactive oxygen species-induced activation of the MAP kinase signaling pathways. Antioxid. Redox Signal. 8, 1775–1789.
Mosmann, T., 1983. Rapid colorimetric assay for cellular growth and survival: application to proliferation and cytotoxicity assays. J. Immunol. Methods 65, 55–63.
Nanotechnology, 2010. Nanotechnology in Health Care: US Industry Study with Forecasts for 2014 & 2019. http://www.freedoniagroup.com/brochure/26xx/2622smwe.pdf.
Oberdorster, G., Oberdorster, E., Oberdorster, J., 2005. Nanotoxicology: an emerging discipline evolving from studies of ultrafine particles. Environ. Health Perspect. 113, 823–839.
Olive, P.L., Frazer, G., Banath, J.P., 1993. Radiation-induced apoptosis measured in Tk6-human B-lymphoblast cells using the comet assay. Radiat. Res. 136, 130–136.
Park, E.J., Park, K., 2009. Oxidative stress and pro-inflammatory responses induced by silica nanoparticles in vivo and in vitro. Toxicol. Lett. 184, 18–25.
Patel, P., Kansara, K., Shah, D., Vallabani, N.V., Shukla, R.K., Singh, S., Dhawan, A., Kumar, A., 2014. Cytotoxicity assessment of ZnO nanoparticles on human epidermal cells. Mol. Cytogenet. 7 (Suppl. 1), 81.
Prach, M., Stone, V., Proudfoot, L., 2013. Zinc oxide nanoparticles and monocytes: impact of size, charge and solubility on activation status. Toxicol. Appl. Pharmacol. 266, 19–26.
Premanathan, M., Karthikeyan, K., Jeyasubramanian, K., Manivannan, G., 2011.

Selective toxicity of ZnO nanoparticles toward gram-positive bacteria and cancer cells by apoptosis through lipid peroxidation. Nanomed. Nanotechnol. Biol. Med. 7, 184–192.
Raingeaud, J., Gupta, S., Rogers, J.S., Dickens, M., Han, J., Ulevitch, R.J., Davis, R.J., 1995. Pro-inflammatory cytokines and environmental stress cause p38 mitogen-activated protein kinase activation by dual phosphorylation on tyrosine and threonine. J. Biol. Chem. 270, 7420–7426.
Rasmussen, J.W., Martinez, E., Louka, P., Wingett, D.G., 2010. Zinc oxide nanoparticles for selective destruction of tumor cells and potential for drug delivery applications. Expert Opin. Drug Deliv. 7, 1063–1077.
Roux, P.P., Blenis, J., 2004. ERK and p38 MAPK-activated protein kinases: a family of protein kinases with diverse biological functions. Microbiol. Mol. Biol. Rev. 68, 320–344.
Roy, R., Tripathi, A., Das, M., Dwivedi, P.D., 2011. Cytotoxicity and uptake of zinc oxide nanoparticles leading to enhanced inflammatory cytokines levels in murine macrophages: comparison with bulk zinc oxide. J. Biomed. Nanotechnol. 7, 110–111.
Sharma, V., Kumar, A., Dhawan, A., 2012. Nanomaterials: exposure, effects and toxicity assessment. Proc. Natl. Acad. Sci. India Sect. B Biol. Sci. 82, 3–11.
Sharma, V., Shukla, R.K., Saxena, N., Parmar, D., Das, M., Dhawan, A., 2009. DNA damaging potential of zinc oxide nanoparticles in human epidermal cells. Toxicol. Lett. 185, 211–218.
Sharma, V., Singh, S.K., Anderson, D., Tobin, D.J., Dhawan, A., 2011. Zinc oxide nanoparticle induced genotoxicity in primary human epidermal keratinocytes. J. Nanosci. Nanotechnol. 11, 3782–3788.
Shukla, R.K., Kumar, A., Gurbani, D., Pandey, A.K., Singh, S., Dhawan, A., 2013. TiO2 nanoparticles induce oxidative DNA damage and apoptosis in human liver cells. Nanotoxicology 7, 48–60.
Singh, N.P., McCoy, M.T., Tice, R.R., Schneider, E.L., 1988. A simple technique for quantitation of low levels of DNA damage in individual cells. Exp. Cell. Res. 175, 184–191.
Suzuki, H., Toyooka, T., Ibuki, Y., 2007. Simple and easy method to evaluate uptake potential of nanoparticles in mammalian cells using a flow cytometric light scatter analysis. Environ. Sci. Technol. 41, 3018–3024.
Tice, R.R., Agurell, E., Anderson, D., Burlinson, B., Hartmann, A., Kobayashi, H., Miyamae, Y., Rojas, E., Ryu, J.C., Sasaki, Y.F., 2000. Single cell gel electrophoresis/Comet assay: guidelines for in vitro and in vivo genetic toxicology testing. Environ. Mol. Mutagen. 35, 206–221.
Totsuka, Y., Ishino, K., Kato, T., Goto, S., Tada, Y., Nakae, D., Watanabe, M., Wakabayashi, K., 2014. Magnetite nanoparticles induce genotoxicity in the lungs of mice via inflammatory response. Nanomaterials 4, 175–188.
Wang, L., O'Donoghue, M.B., Tan, W., 2006. Nanoparticles for multiplex diagnostics and imaging. Nanomedicine 1, 413–426.
Xia, T., Kovochich, M., Liong, M., Madler, L., Gilbert, B., Shi, H., Yeh, J.I., Zink, J.I., Nel, A.E., 2008. Comparison of the mechanism of toxicity of zinc oxide and cerium oxide nanoparticles based on dissolution and oxidative stress properties. ACS Nano 2, 2121–2134.
Zolnik, B.S., Gonzalez-Fernandez, A., Sadrieh, N., Dobrovolskaia, M.A., 2010. Minireview: nanoparticles and the immune system. Endocrinology 151, 458–465.